


RESEARCH

Open Access



# Single-cell RNA sequencing analysis of the temporomandibular joint condyle in 3 and 4-month-old human embryos

Qianqi Zhu<sup>1†</sup>, Miaoying Tan<sup>1†</sup>, Chengniu Wang<sup>3†</sup>, Yufei Chen<sup>3</sup>, Chenfei Wang<sup>1</sup>, Junqi Zhang<sup>1</sup>, Yijun Gu<sup>1</sup>, Yuqi Guo<sup>1</sup>, Jianpeng Han<sup>1</sup>, Lei Li<sup>1</sup>, Rongrong Jiang<sup>1</sup>, Xudong Fan<sup>1</sup>, Huimin Xie<sup>1</sup>, Liang Wang<sup>1</sup>, Zhifeng Gu<sup>2\*</sup>, Dong Liu<sup>4\*</sup>, Jianwu Shi<sup>3\*</sup> and Xingmei Feng<sup>1\*</sup> 

## Abstract

**Background** The temporomandibular joint (TMJ) is a complex joint consisting of the condyle, the temporal articular surface, and the articular disc. Functions such as mastication, swallowing and articulation are accomplished by the movements of the TMJ. To date, the TMJ has been studied more extensively, but the types of TMJ cells, their differentiation, and their interrelationship during growth and development are still unclear and the study of the TMJ is limited. The aim of this study was to establish a molecular cellular atlas of the human embryonic temporomandibular joint condyle (TMJC) by single-cell RNA sequencing, which will contribute to understanding and solving clinical problems.

**Results** Human embryos at 3 and 4 months of age are an important stage of TMJC development. We performed a comprehensive transcriptome analysis of TMJC tissue from human embryos at 3 and 4 months of age using single-cell RNA sequencing. A total of 16,624 cells were captured and the gene expression profiles of 15 cell clusters in human embryonic TMJC were determined, including 14 known cell types and one previously unknown cell type, "transition state cells (TSCs)". Immunofluorescence assays confirmed that TSCs are not the same cell cluster as mesenchymal stem cells (MSCs). Pseudotime trajectory and RNA velocity analysis revealed that MSCs transformed into TSCs, which further differentiated into osteoblasts, hypertrophic chondrocytes and tenocytes. In addition, chondrocytes (CYTL1<sup>high</sup> + THBS1<sup>high</sup>) from secondary cartilage were detected only in 4-month-old human embryonic TMJC.

**Conclusions** Our study provides an atlas of differentiation stages of human embryonic TMJC tissue cells, which will contribute to an in-depth understanding of the pathophysiology of the TMJC tissue repair process and ultimately help to solve clinical problems.

**Keywords** TMJC, Human embryonic cells, Cellular transcriptomics, Gene expression

<sup>†</sup>Qianqi Zhu, Miaoying Tan and Chengniu Wang have contributed equally to this work.

\*Correspondence:

Zhifeng Gu

guzf@ntu.edu.cn

Dong Liu

liudongtom@gmail.com

Jianwu Shi

jwshi@ntu.edu.cn

Xingmei Feng

xingmeifeng@ntu.edu.cn

Full list of author information is available at the end of the article



## Background

During human embryonic development, abnormal development of the TMJC cartilage can lead to malformation of the oral and maxillofacial system, and abnormal respiratory and masticatory functions [1, 2]. Dysplasia development of the TMJ during the embryonic period may even lead to the development of congenital TMJ disorders. The TMJ is a complex joint that including the condyle, temporal articular surface, and the articular disc [1, 3]. Functions such as mastication, swallowing, and articulation are accomplished through TMJ movements [2, 4].

The embryonic development of human TMJ can be divided into three important stages: 1. the initial stage (8–9 weeks), the temporal and condylar embryonic bases appear, the condylar embryonic base begins intrachondral osteogenesis; 2. the differentiation stage (10–20 weeks), the articular disc, joint cavity and synovial membrane are formed, secondary cartilage appears, the condyle further endochondral osteogenesis; 3. The completion stage (21 weeks to delivery), the components of the TMJ have formed, Meckel's cartilage disappears, the articular disc is further modified, the condyle continues endochondral osteogenesis, endochondral osteogenesis occurs in the articular fossa, and haematopoietic tissue appears. Of these, the differentiation phase (10–20 weeks) is crucial for the development of the condylar tissue of the TMJ [2, 5]. A single-cell atlas of the condylar tissue of human embryos at three and four months of age was constructed. To our knowledge, this is the first and earliest single-cell atlas of human embryonic TMJ condylar tissue.

Single-cell RNA sequencing had been widely used in the study of joints. In the mouse knee joint, combining segmental bulk- and single-cell RNA sequencing were used to define the chondrocyte gene expression signature [6]. Single-cell RNA sequencing was used to comparing major cell clusters in osteoarthritic, Kashin-Beck disease and healthy articular chondrocytes [7]. Single-cell RNA sequencing has shown that different subpopulations of synovial fibroblasts exist in patients with rheumatoid arthritis (RA) [8]. Single-cell RNA sequencing revealed the transcriptomic changes in subchondral bone hypoplasia of the knee and in cartilage after traumatic fracture [9]. Single-cell RNA sequencing has also identified transcriptome heterogeneity and early molecular changes associated with post-traumatic osteoarthritis in mouse articular chondrocytes [10]. However, studies of single-cell RNA sequencing of the TMJ, particularly in human embryos, have not been reported.

Many key genes and transcription factors were reported to be involved in the differentiation of chondrocytes and osteoblasts. The common mesenchymal

progenitors cell of chondrocytes and osteoblasts can express *Sox9* and *Runx2* [11]. The direction of cell differentiation toward chondrocytes or osteoblasts depends on the expression of *Sox9* and *Runx2* [12]. *Sox9* regulates the chondrocytes differentiation [13]. *Runx2* is expressed in hypertrophic chondrocytes and promotes the expression of *Col10a1* and *Mmp13* [14]. *Runx2* also promotes osteoblast differentiation by regulating the expression of *Osx* [15]. *Osx* transactivates *Col1a1*, which is essential for the differentiated osteoblasts. Therefore, *Osx* is essential for the differentiation of preosteoblastic cells [15]. Moreover, many signaling pathways have been reported to be involved in the differentiation of bone cells. The Indian Hedgehog (IHH) signaling pathway promotes chondrocyte differentiation toward hypertrophic terminal [16]. Conversely, the parathyroid hormone-related peptide (PTHrP) signaling pathway prevents premature chondrocyte differentiation [17]. In the previous studies, many other signaling pathways including PTN [18], BMP [19], FGF [20], CXCL [21], MSTN [22] and GH [23] have been associated with chondrocyte and osteoblast differentiation. In conclusion, the exploration of key genes, transcription factors and signaling pathways is important for understanding the development and differentiation of human embryonic TMJC cells.

In recent years, single-cell sequencing techniques have been used to study the cell types of tissues and the differentiation relationships between cell clusters. To study the cell types and differentiation relationships of human embryonic TMJC, we completed single-cell sequencing of TMJC from 3- and 4-month-old human embryos. To the best of our knowledge, this is the first and earliest single-cell atlas of human embryonic TMJC. In this study, we describe the cell types and differentiation relationships of human embryonic TMJC tissue. This has important implications for studying the functional and differentiation relationships of cell clusters and the congenital TMJ diseases caused by abnormal development of human embryonic TMJC.

## Results

### scRNA-Seq analysis of human embryonic TMJC cell types

To construct a cellular atlas of the human embryonic TMJC in 3 and 4-month-old, we isolated TMJC tissue from two early developmental stages: 7052 cells from 3-month-old TMJC and 9572 cells from 4-month-old TMJC. After cell quality control (Additional file 1: Fig. S1b), a total of 16,624 cells were clustered into 15 cell clusters. We annotated these 15 cell clusters to include satellite cells, MSCs, TSCs, tenocytes, myoblasts, endothelial cells, hypertrophic chondrocytes, erythrocytes, proliferating cells, leukocytes, pericytes, chondrocytes (CYTL1<sup>high</sup> + THBS1<sup>high</sup>), schwann's cells,

osteoblasts and osteoclasts (Fig. 1a and Additional file 1: Fig. S5). Unexpectedly, we found no chondrocytes cluster from secondary cartilage in the 3-month-old TMJC. However, a distinct cluster of chondrocytes (CYTL1<sup>high</sup>+THBS1<sup>high</sup>) from secondary cartilage appeared in 4-month-old TMJC (Fig. 1b and Additional file 1: Fig. S1c). The marker genes used for annotation are shown (Additional file 1: Fig. S1d and Additional file 1: Fig. S6). The expression of CYTL1 and THBS1 as marker genes for chondrocytes clustering is illustrated (Fig. 1c). Immunofluorescence staining showed that CYTL1 and THBS1 were expressed in 4-month-old TMJC. CYTL1 and THBS1 were not detected in 3-month-old TMJC (Fig. 1d). The top 5 DEGs in each cluster are shown (Additional file 1: Fig. S1e). The GO analysis for each cluster is also shown (Additional file 1: Fig. S1f).

Marker genes used to annotate hypertrophic chondrocytes included COL10A1, MMP13, RUNX2, FGF2 and SCIN (Additional file 2: Fig. S2a, 2b). Immunofluorescence staining showed FGF2 and SCIN were expressed in hypertrophic chondrocytes from 3-month-old and 4-month-old TMJC (Additional file 2: Fig. S2c).

#### Subpopulation analysis of TSCs

In this study, we identified TSCs as a specific cell cluster. Subpopulation analysis revealed that TSCs consisted of 5 subpopulations (Fig. 2a). The proportions of the subpopulations were osteoblasts (67.9%), preosteoblasts (19.0%), hypertrophic chondrocytes (7.1%), chondrocytes (3.0%) and MSCs (2.9%) (Fig. 2b). Five subpopulations were annotated on the reported cell markers (Additional file 1: Fig. S1g). As marker genes, CAPN6 expression in MSCs and PTN expression in TSCs are illustrated separately (Fig. 2c, d). Immunofluorescence staining showed no colocalization and expression of CAPN6 and PTN in different cells of 3 and 4-month-old TMJC (Fig. 2e). These results indicate the presence of MSCs and TSCs in 3 and 4-month-old TMJCs. These results also further confirm that MSCs and TSCs are distinct cell types in human embryonic TMJC (Fig. 2e).

#### Monocle3 and RNA velocity analysis of cell differentiation relationships

In order to clarify the differentiation relationships between TMJC cells, 15 TMJC cell clusters were calculated and divided into 8 differentiation trajectories based on Monocle3 analysis. Clear differentiation pathways could be found between MSCs, TSCs, tenocytes, hypertrophic chondrocytes and osteoblasts (Additional file 3: Fig. S3a). We further focused on the differentiation relationships between these five cell clusters. It is reasonable to designate the MSC cluster as the root in the pseudotime trajectory pathway. The differentiation

relationships between these five cell clusters were identified. MSCs were positioned as the origin and differentiated into TSCs. TSCs could further differentiate into tenocytes, hypertrophic chondrocytes and osteoblasts, respectively (Fig. 3a). Pseudotime analysis of 3- and 4-month-old TMJC cells is also shown (Additional file 3: Fig. S3c). In addition, we used RNA velocity analysis to look at the extent and orientation of MSCs, TSCs, tenocytes, hypertrophic chondrocytes and osteoblasts. The arrow directions showed that MSCs and TSCs are highly heterogeneous and are thought to be the starting point for differentiation in each direction. The arrowheads of the tenocytes, hypertrophic chondrocytes and osteoblasts are oriented in the same direction, indicating that these three clusters have a stable state and appear to differentiate from the TSCs (Fig. 3b). RNA velocity analysis of 15 TMJC cell clusters and 5 cell clusters from 3- and 4-month-old TMJCs are also shown (Additional file 3: Fig. S3b, d), and these results are consistent with the monocle3 analysis. Expression of key genes associated with chondrocyte and osteoblast differentiation were illustrated. These genes included RUNX2, SOX9, MMP13, SOST, VEGFA, COL10A1, MAF, CCDC80, and SYNE2 (Fig. 3c).

#### CellChat analysis of signaling pathways in cell cluster differentiation

To analyze cell–cell interactions and potential signaling pathways, we screened known cell–cell exchanges using CellChat. Complex networks of cell–cell interactions were identified in 15 cell clusters (Fig. 4a and Additional file 4: Fig. S4a). Notably, the FGF signaling pathway inferred by CellChat was highly enriched in MSCs, TSCs, hypertrophic chondrocytes, osteoblasts and tenocytes (Fig. 4b and Additional file 4: Fig. S4b). We further identified FGF7-FGFR1 as a major contributor to the FGF signaling pathway (Fig. 4c). We further investigated the expression of molecules involved in FGF7-FGFR1 and found that FGFR1 was mainly expressed in TSCs, tenocytes, hypertrophic chondrocytes and osteoblasts (Additional file 4: Fig. S4c). Thus, FGF7-FGFR1 is the main signaling pathway mediating cell–cell communication between MSCs, TSCs, hypertrophic chondrocytes, osteoblasts and tenocytes (Fig. 4d and Additional file 4: Fig. S4d). In addition, we also demonstrated the other key signaling pathways with the function of “identify Communication Patterns” in CellChat. Among the patterns of outgoing communication in secretory cells, TSCs, hypertrophic chondrocytes and osteoblasts belong to pattern 1. Pattern 1 contains PTN, THBS, ANGPTL, FGF, TENASCIN, CHAD, CADM, CDH, BSP, BMP, HSPG, OSM, ncWNT, RANKL, ACTIVIN, SEMA4, IL16, and DMP1 and other signaling pathways. Meanwhile, incoming

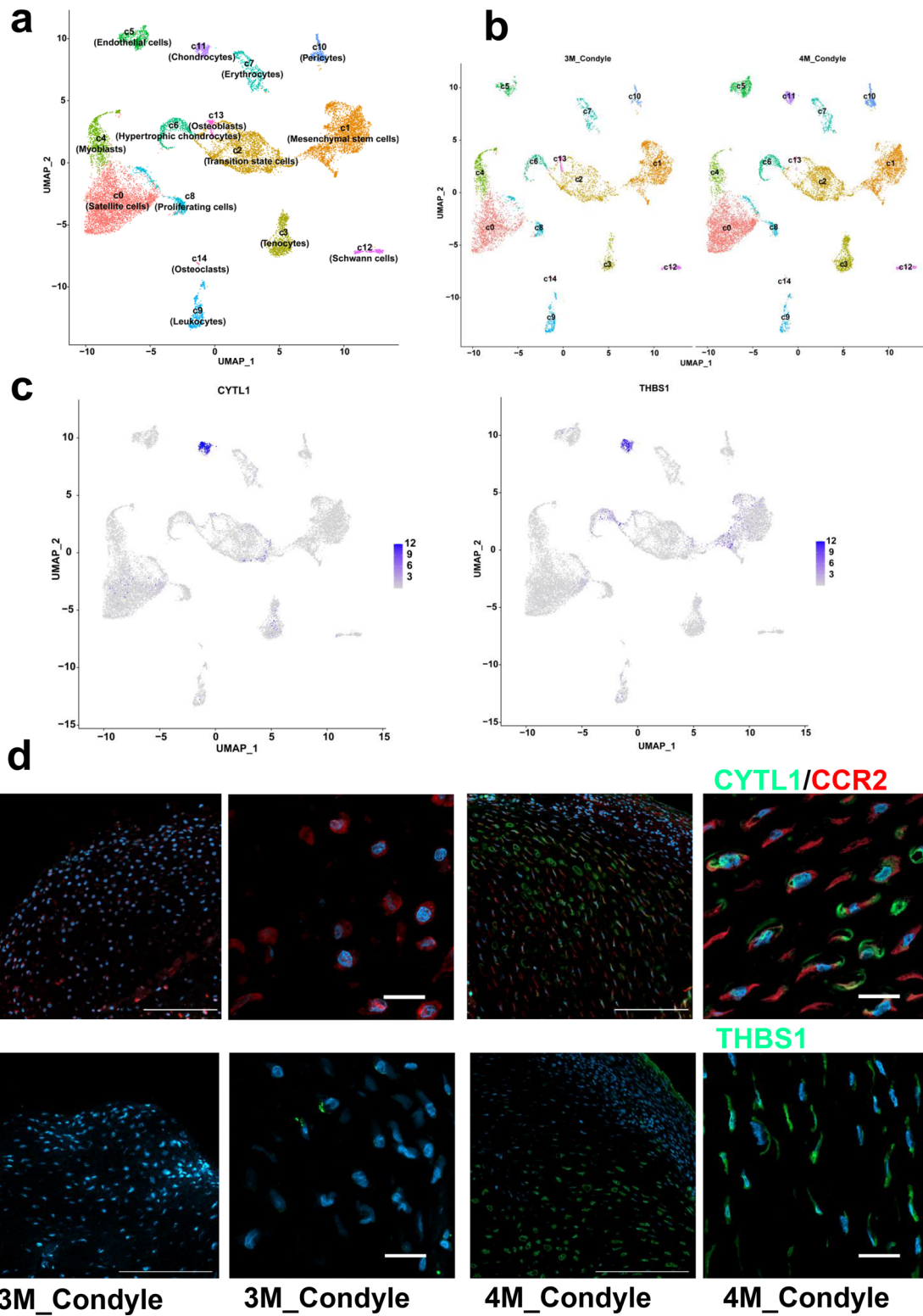


**Fig. 1** Overview of the scRNA sequencing of human embryonic TMJC. **a** The 15 cell clusters identified in human embryonic TMJC using UMAP. **b** The cell clusters were identified in 3 and 4-month-old human embryonic TMJC. **c** The expression of CYTL1 and THBS1 in each cluster of human embryonic TMJC. **d** The immunofluorescent staining of CYTL1 and THBS1 in 3 and 4-month-old human embryonic TMJC, Scale bar = 1 mm and 50  $\mu$ m

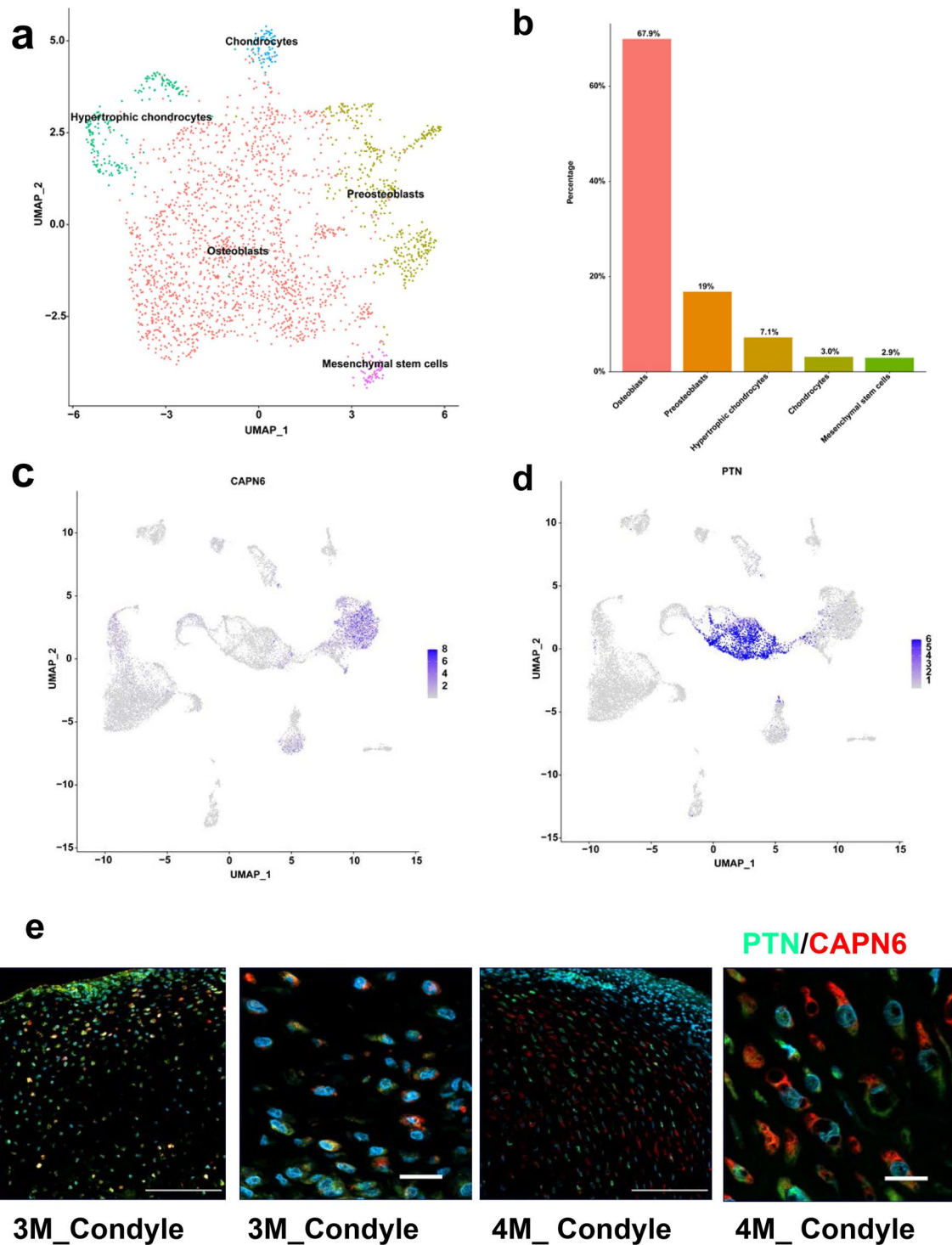


**Fig. 2** Subpopulation analysis of TSCs. **a** The five subpopulations of TSCs were visualized using UMAP. **b** The cell proportions of subpopulations in TSCs. **c** The expression of CAPN6 in each cluster of human embryonic TMJC. **d** The expression of PTN in each cluster of human embryonic TMJC. **e** Immunofluorescence staining of CAPN6 and PTN in 3 and 4-month-old human embryonic TMJC, Scale bar = 1 mm and 50  $\mu$ m

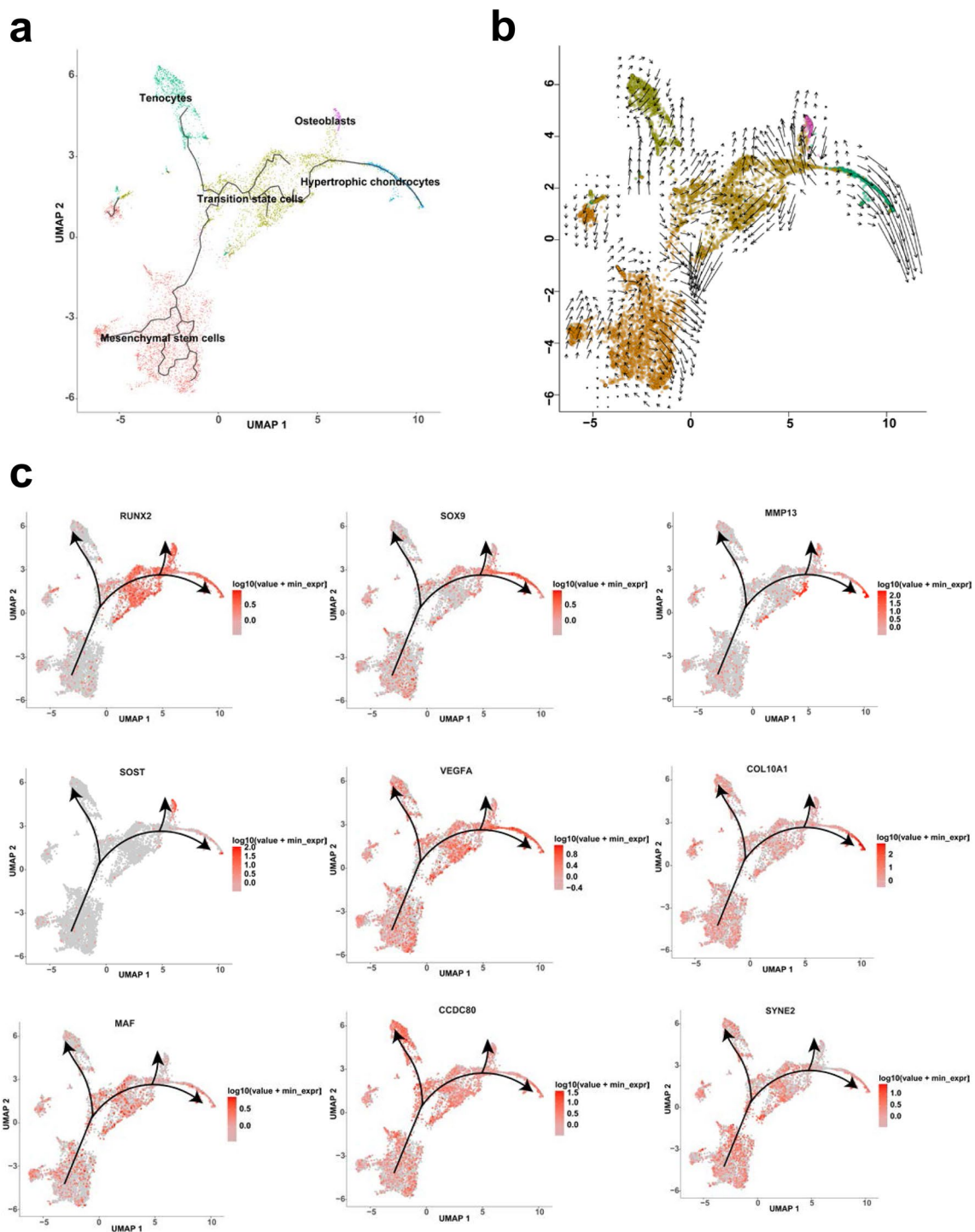


**Fig. 3** The differentiation relationship analysis of MSCs, TSCs, tenocytes, hypertrophic chondrocytes and osteoblasts. **a** The differentiation relationship among MSCs, TSCs, tenocytes, hypertrophic chondrocytes and osteoblasts based on Monocle3 analysis. **b** The differentiation relationship among these five clusters based on RNA velocity analysis. **c** The expression of key genes including RUNX2, SOX9, MMP13, SOST, VEGFA, COL10A1, MAF, CCDC80 and SYNE2 among the five clusters

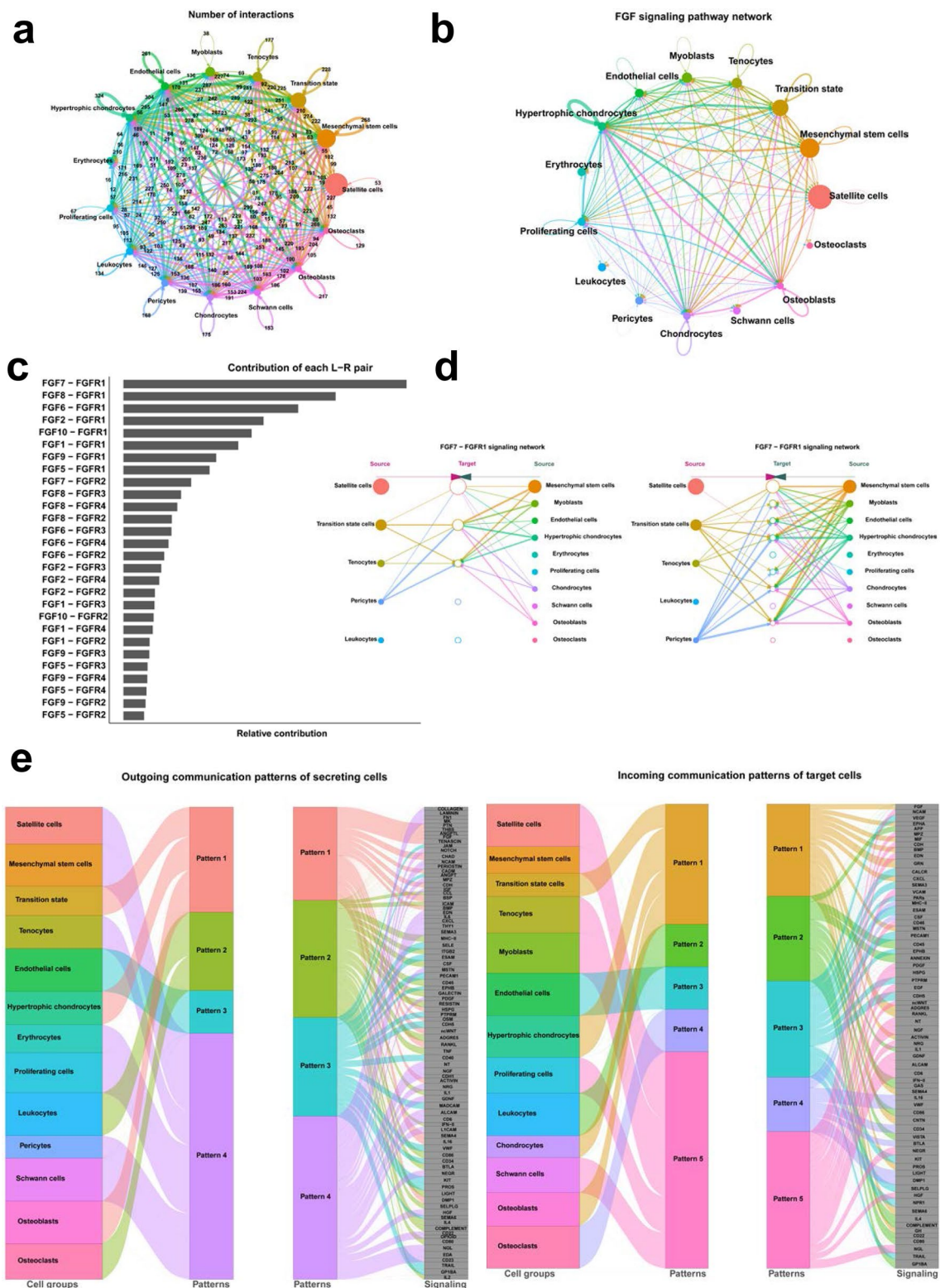


**Fig. 4** CellChat analysis of human embryonic TMJC clusters. **a** The number of ligand-receptor pairs in 15 cell clusters. **b** FGF signaling pathway networks among 15 cell clusters. **c** The contribution of each ligand-receptor pairs of FGF signaling pathway. **d** FGF7-FGFR1 signaling pathway networks among 15 cell clusters. **e** The analysis of outgoing communication patterns of secreting cells and incoming communication patterns of target cells among 15 cell clusters

communication patterns of target cells indicated that TSCs, hypertrophic chondrocytes and osteoblasts were in pattern 1, regulated by FGF, EPHA, MIF, BMP, GRN, CXCL, MSTN, ADGRE5, RANKL, ACTIVIN, SEMA4, CNTN, PROS, SEMA6 and GH (Fig. 4e and Additional file 4: Fig. S4e).

#### Analysis of transcription factors in cells cluster differentiation

Figure 5a shows the activity matrix of binary regulators. SP9, SHOX2, TBX18, PLAGL1, PAX9 and SRY are turned on in MSCs. TCF7, DLX6, BCL11A, PRRX2 and MSX1 are turned on in TSCs. MKX, ETV4, DLX1, ALX4 and USF1 are turned on in tenocytes. FOXA2, TRPS1, SOX6, SIX3 and FOXA3 are turned on in hypertrophic chondrocytes. ZBTB7C, DLX3, IRX5 and TBX2 are turned on in osteoblasts. Strikingly, all 483 regulons were organized into 13 modules. Representative regulators and cell clusters were identified in each module. For example, module 3 consisted of hypertrophic chondrocytes and chondrocytes, containing regulons of ERE, BHL, HE41, FOXC1, HE40 and ATF2. Module 5 was organized by MSCs and TSCs and included ZNF607, MSX1, ZNF157, GLI2 and ALX4. Module 10 consisted of hypertrophic chondrocytes and osteoblasts, containing regulators of PHOX2A, ESRRA, PGAM2 and SOX8 (Fig. 5c). The heatmap shows that many common regulators are turned on between MSCs and TSCs (Fig. 5b). Interaction mapping of transcription factor networks showed that PAX1 and PAX9 are important regulators of chondrocyte differentiation and are commonly switched on between MSCs and TSCs. NRF1, TFEB, ALX4 and DLX2 are associated with the differentiation of MSCs into osteoblasts and also commonly switched on between MSCs and TSCs. In addition, sequences of promoter regions of transcription factors were shown to target genes, including PAX1, PAX9, NRF1, TFEB, ALX4 and DLX2 (Fig. 5d).

#### Discussion

During the embryonic period, the development of the TMJ lags behind that of other joints [24]. As a result, at birth, the TMJ remains largely immature. Developmental disorders of the TMJ such as hypoplasia and aplasia are characterized by TMJ dysfunction [25]. In addition, there are many causes of TMJ growth disorders and abnormalities. Growth disorders of TMJ development may occur in utero and lead to contributions such as hyperplasia or hypoplasia of the TMJ. Congenital abnormalities of the TMJ can be divided into three categories, including hypoplasia or aplasia of the TMJ, hyperplasia and bifidity [24, 26]. It is important to study the development of

the condyle for treating congenital abnormalities of the condyle.

Single-cell RNA sequencing was used to identify new cell clusters and cell function in the joint. Seven clusters of articular chondrocytes in human OA cartilage have been identified by single-cell RNA sequencing [27]. Different subtypes of cells, particularly macrophages, have been shown to have pro- or anti-inflammatory effects in the joint depending on polarization [28, 29]. In patients with rheumatoid arthritis (RA), 13 distinct cell subpopulations were identified within the synovium by single-cell RNA sequencing [30]. In the adult knee synovium, the Gdf5-lineage cell cluster contains fibroblasts that become pathogenic in inflammatory arthritis [31]. In the articular cartilage of the knee joint of healthy mice, nine chondrocyte subtypes were identified by single-cell RNA sequencing [10]. Single-cell RNA sequencing was used to determine the differentiation trajectory and molecular regulation of fibroblast and progenitor cell clusters in the synovial membrane of knee joints of steady-state and injured mouse knees [32]. In addition to the common cell populations of Osteoblast, Chondrocyte, Tenocyte, there are cell population difference between the synovial membrane of the knee joints and TMJC.

To better understand the cell types and differentiation relationships of the human embryonic TMJC, we constructed a cellular atlas of the 3- and 4-month-old TMJC by single-cell sequencing. In previous reports, many studies have revealed the development of TMJ through imaging and morphological studies [5]. To date, there have been no studies on the cellular level of the human embryonic TMJC. This is the first and earliest atlas of the cellular development of the human embryonic TMJC. We have identified 15 cell clusters (Fig. 1a). We found that the chondrocytes cluster (CYTL1<sup>high</sup> + THBS1<sup>high</sup>) was not yet differentiated in 3-month-old TMJC. However, a distinct chondrocytes population emerged in 4-month-old TMJC (Fig. 1b and Additional file 1: Fig. S1c). We therefore, hypothesize that chondrocytes have differentiated in 4-month-old TMJC. Chondrocytes differentiate later than other cell clusters, suggesting that chondrocytes differentiation is completed at a later stage of TMJC development. This phenomenon is the first to be reported in the development of human embryonic TMJC.

We identified TSCs as a new cell cluster that can be divided into five subpopulations including osteoblasts, preosteoblasts, hypertrophic chondrocytes, chondrocytes and MSCs (Fig. 2a). The different composition of TSCs suggests that TSCs possess multiple differentiation potentials. Based on this prediction, three new differentiation lineages related to TSCs were proposed by trajectory and RNA velocity analysis. MSCs differentiate into TSCs. TSCs can further differentiate into



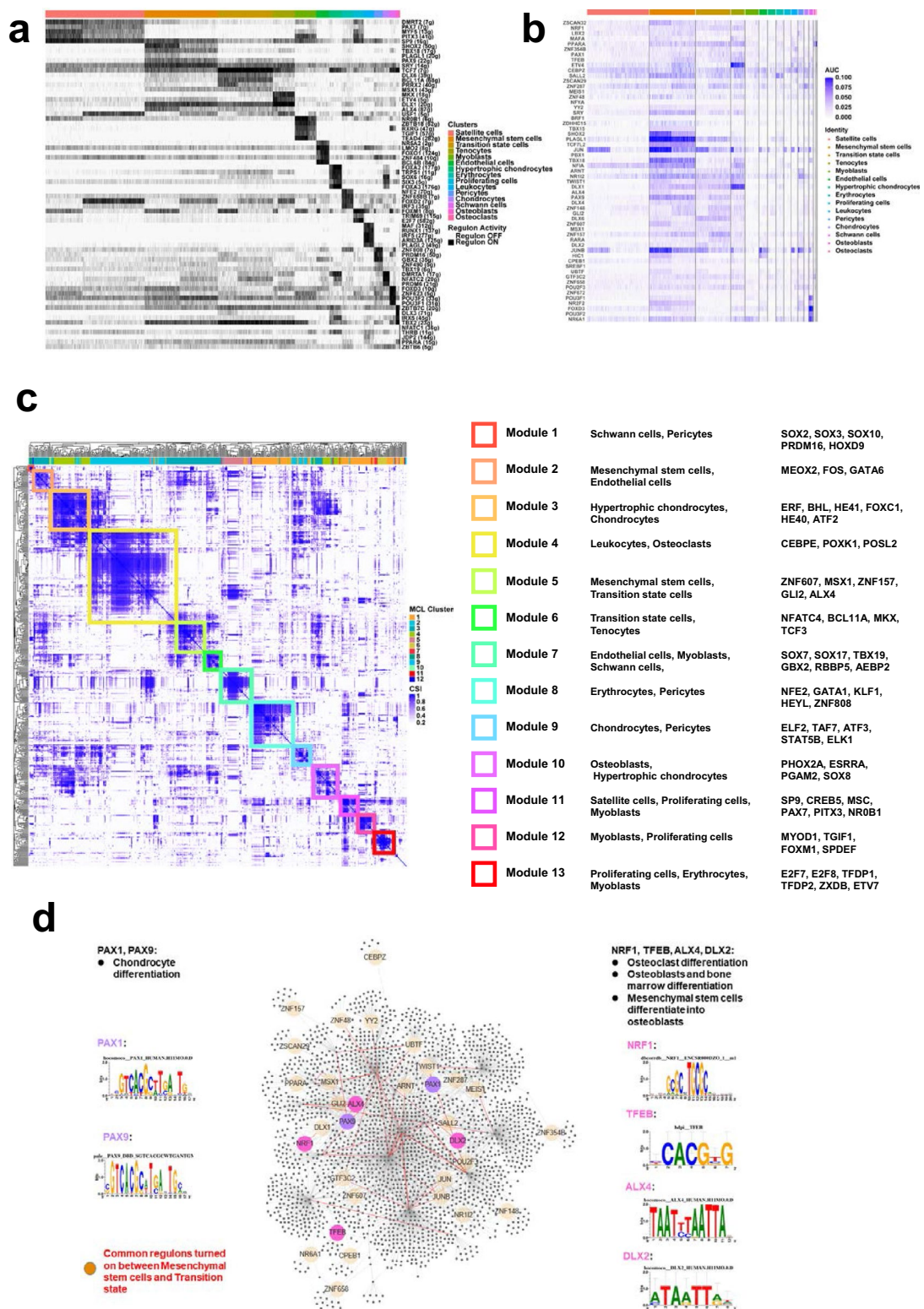


**Fig. 5** Transcription factors analysis among human embryonic TMJC clusters. **a** The regulon activity analysis showed the on/off of the specific regulons in each cluster. **b** Heatmap showed the common regulons were turned on between MSCs and TSCs. **c** Modules analysis of cell clusters and common regulons. **d** Interaction mapping of transcription factors networks showed common regulons between MSCs and TSCs

hypertrophic chondrocytes, osteoblasts and tenocytes (Fig. 3a, b). MSCs have been reported to differentiate into tenocytes [33]. Contrast to previous reports [33], tenocytes were not differentiated directly from MSCs, but from TSCs from human embryonic TMJC (Fig. 3a). The stature-deficient homeobox 2 (*Shox2*) has been reported to be expressed in the developing TMJ. Overexpression of *Shox2* will result in congenital hypoplasia in the TMJ in mice. Furthermore, deletion of *Shox2* also leads to hypoplasia in the TMJ of mice. In our study, SHOX2 was specially expressed in MSCs of human embryonic TMJC. These results suggest that SHOX2 plays an important role in the function and early differentiation of the MSCs in human embryonic TMJC. During development, hypertrophic chondrocytes and osteoblasts have been reported as separate cell lines [11]. They are differentiated from osteochondro-progenitors cells. *Sox9* and *Runx2* are highly expressed in osteochondro-progenitors cells [34]. In the present study, similar to osteochondro-progenitors, TSCs highly expressed *Sox9* and *Runx2* and were able to differentiate into hypertrophic chondrocytes and osteoblasts, respectively (Fig. 3c). In addition, RUNX2 [35] has been reported to be involved in the trans-differentiation of chondrocytes to osteoblasts and to promoted osteoblast differentiation. RUNX2 is highly expressed in the differentiation pathways from TSCs to hypertrophic chondrocytes and from TSCs to osteoblasts. SOX9 has been reported to be a key transcriptional regulator of chondrogenesis [36]. MMP13 has been implicated in osteogenesis [37]. SOX9 and MMP13 are highly expressed in the differentiation of TSCs to hypertrophic chondrocytes. SOST has been implicated in the differentiation of bone formation [38]. In the present study, SOST was highly expressed in osteoclasts. Other key genes include VEGFA [39], COL10A1 [40], MAF [41], CCDC80 [42] and SYNE2 [43] which are associated with bone proliferation and differentiation and are widely expressed in MSCs, TSCs, tenocytes, hypertrophic chondrocytes and osteoblasts. These results suggest the key genes associated with the differentiation of chondrocytes and osteoblasts are expressed in the TMJC clusters (Fig. 3c). These genes can promote the differentiation of human embryonic TMJC cells. Interestingly, we found that TSCs also have the potential ability to differentiate into tenocytes. Thus, as intermediate cells, between MSCs and other cell clusters, TSCs are critical for the development of human embryonic TMJCs. Although we have established the presence of TSCs in the human embryonic TMJC (Fig. 2e), further experiments are required to reveal their detailed functions.

We performed an analysis of cell–cell communication between the TMJC cell clusters. We found that the FGF signaling pathway mediated the communication

between these five clusters (Fig. 4b). We then analyzed the strength of the FGF signaling pathway and found that FGF7-FGFR1 was the main pathway (Fig. 4c, d). FGF7 has been reported to promote bone formation by increasing osteogenesis [44]. FGF7 also promotes osteogenic differentiation by regulating the expression of the  $\beta$ -catenin and Runx2 signaling pathways [45]. In the present study, as a source cell cluster, TSCs communicated with target cell cluster of MSCs via the FGF7-FGFR1 signaling pathway. In addition, as source cell clusters, hypertrophic chondrocytes, osteoblasts and tenocytes also communicate with the target cell clusters of TSCs via the FGF7-FGFR1 signaling pathway, respectively. Thus, as the primary signaling pathway, we determined that FGF7-FGFR1 mediated the communication and differentiation among MSCs, TSCs, hypertrophic chondrocytes, osteoblasts and tenocytes. In addition, we explored other signaling pathways between TSCs, hypertrophic chondrocytes and osteoblasts. Notably, we screened many chondrocyte and osteoblast differentiation signaling pathways, including PTN [18], BMP [19], TENASCIN [46], ACTIVIN [47], RANKL [47], DMP1 [48], MK [49], FGF [20], GRN [50], CXCL [21], MSTN [22] and GH [23]. These reported signaling pathways regulating bone differentiation may also play an important role in the differentiation of TSCs, hypertrophic chondrocytes and osteoblasts. In addition, we screened other signaling pathways including THBS, ANGPTL, CHAD, CADM, CDH, BSP, HSPG, OSM, ncWNT, SEMA4, IL16, which also mediate cellular communication in TSCs, hypertrophic chondrocytes and osteoblasts (Fig. 4e). The role of these signaling pathways in cell differentiation is elusive and needs to be further explored.

In addition to cell–cell communication analysis, transcription factor analysis revealed that some specific transcription factors were turned on in the cell clusters (Fig. 5a). For example, SHOX2 [51], TBX18 [52] and PAX9 [53], which are associated with ossification and chondroitin differentiation, are turned on in MSCs. TCF7 [20], DLX6 [54] and MSX1 [55], which are reported to be involved in ossification and chondroitin differentiation, are turned on in TSCs. MKX [56] which is associated with tenocytes differentiation, is turned on in tenocytes. FOXA2 [57], TRPS1 [58], SOX6 [59] and FOXA3 [60], which are associated with chondrocyte differentiation and hypertrophy, are turned on in hypertrophic chondrocytes. DLX3 [61] and IRX5 [62] which are associated with the ossification and differentiation, are turned on in osteoblasts. These results suggest that transcription factors that are specifically switched on are essential for maintaining specific functions of the cell cluster. Furthermore, module analysis revealed that common regulatory factors were switched on in different cell clusters (Fig. 5c). For

example, Module 3 consists of hypertrophic chondrocytes and chondrocytes containing common regulators of ERF [63], FOXC1 [64] and ATF2 [65] which have been reported to be involved in bone formation and osteogenic differentiation. Module 10 consists of hypertrophic chondrocytes and osteoblasts and contains co-regulators of SOX8 [66] and ESRRA [67] which are important regulators of chondrogenic and osteoblast differentiation (Fig. 5c). Notably, co-regulators including PAX9 [53], SP9 and TCF7 [20, 68] were switched on between MSCs and TSCs. Regulon module analysis showed MSCs and TSCs were in module 5. 32 co-regulators were further switched on between MSCs and TSCs. Among these co-regulators, PAX1 [69] and PAX9 are important regulators of chondrocyte differentiation. NRF1 [70], TFEB [71], ALX4 [72] and DLX2 [73] are associated with the differentiation of MSCs into osteoblasts (Fig. 5d). These co-regulators turned on between MSCs and TSCs may mediate the differentiation from MSCs to TSCs and further to tenocytes, hypertrophic chondrocytes, and osteoblasts, respectively.

## Conclusions

In summary, our data provided the first and earliest cellular atlas of the human embryonic TMJC. The present results show that chondrocytes from secondary cartilage differentiate in 4-month-old TMJC and that chondrocytes differentiate later than other cell clusters. Our results also demonstrated the differentiation relationships and underlying mechanisms of differentiation between MSCs, TSCs, hypertrophic chondrocytes, osteoblasts and tenocytes by advanced analysis of single-cell sequencing (Fig. 6). This study is an indispensable resource for studying the development and differentiation of human embryonic TMJC. Our findings also have important implications for the study of cellular mechanisms of temporomandibular joint disorders (TMD), which are caused by abnormal embryonic development of the TMJC.

## Methods

### Collection of human embryonic TMJC

This work was reviewed and approved by the Institutional Review Boards of Nantong University Hospital (2020-K013). Parents of study participants signed an Informed consent form. For scRNA-seq, TMJC tissue was isolated by surgical excision. The entire mandible, including the mandibular body and TMJ (condyle, joint capsule, joint disc, part of fibrous ligament and temporo-articular fossa), was isolated along the mandibular labiobuccal migration. The mandibular body, condyle and coracoid process were separated from the rest of the TMJ. The condyle is separated from the mandibular body

through the neck of the condyle (Additional file 1: Fig. S1a). The left condyle was cut into pieces as far as possible and placed in tissue preservation solution (Singleron Biotechnologies, Nanjing, China), and then transported to the laboratory by cold chain for cell dissociation and single cell sequencing.

### Preparation of single-cell suspensions

The dissociation of human embryonic TMJC was performed according to a previous study [74]. Briefly, the isolated TMJC tissue was cut into 2–3 mm pieces. Tissue pieces were washed with Hanks Balanced Salt Solution (HBSS). These tissue fragments were spin-digested for 15 using tissue dissociation solution (Singleron Biotechnologies, Nanjing, China). The pieces were filtered through a sterile 40- $\mu$ m filter (Corning, NY, USA) and centrifuged at 150 g for 5 min. Erythrocytes were removed using a lysis reagent (Singleron Biotechnologies, Nanjing, China) for 10 min. Afterwards, cells were resuspended in PBS and stained with trypan blue (T6146, Sigma, Burlington, VT, USA). Cell viability was assessed using a TC20 automated cell counter (Bio-Rad, Hercules, CA, USA).

### Library preparation and data pre-processing

A cell suspension at a concentration of  $1 \times 10^5$  cells/mL of was then added to the microfluidic plate. The scRNA-seq libraries were constructed using the Single-cell RNA Library Kit (Singleron Biotechnologies, Nanjing, China). The constructed libraries were pooled onto an Illumina HiSeq $\times$ 10 sequencer machine for sequencing. Raw reads were processed by the CeleScope (<https://github.com/singleron-RD/CeleScope>) pipeline. First, low quality raw reads and adaptor sequences were trimmed by fastqc (version 0.11.7) and cutadapt (version 1.17). Reads were mapped to GRCm38 (Ensembl V. 92 annotation) using STAR (version 020201). Gene counts and UMI counts were calculated using FeatureCounts (version 1.6.2). A series of analysis procedures were completed by CeleScope and a gene expression matrix was generated.

### Dimension-reduction and clustering analysis

The dimension reduction and cell clustering were performed in R using the Seurat version 4 package (<https://satijalab.org/seurat/>) [75]. Sctransform (SCT) (<https://github.com/ChristophH/sctransform>) was used to remove batch effects and to normalize the expression data. The function of subset was used to extract a subset of in Seurat objects which meet the requirements of quality control ( $nFeature\_RNA > 200$  &  $nFeature\_RNA < 4000$  &  $percent.mt < 50$  &  $nCount\_RNA < 20,000$ ). The low-quality cells were filtered out and did not participate in the downstream data analysis. The first 3000 variable genes were selected for sample data integration.

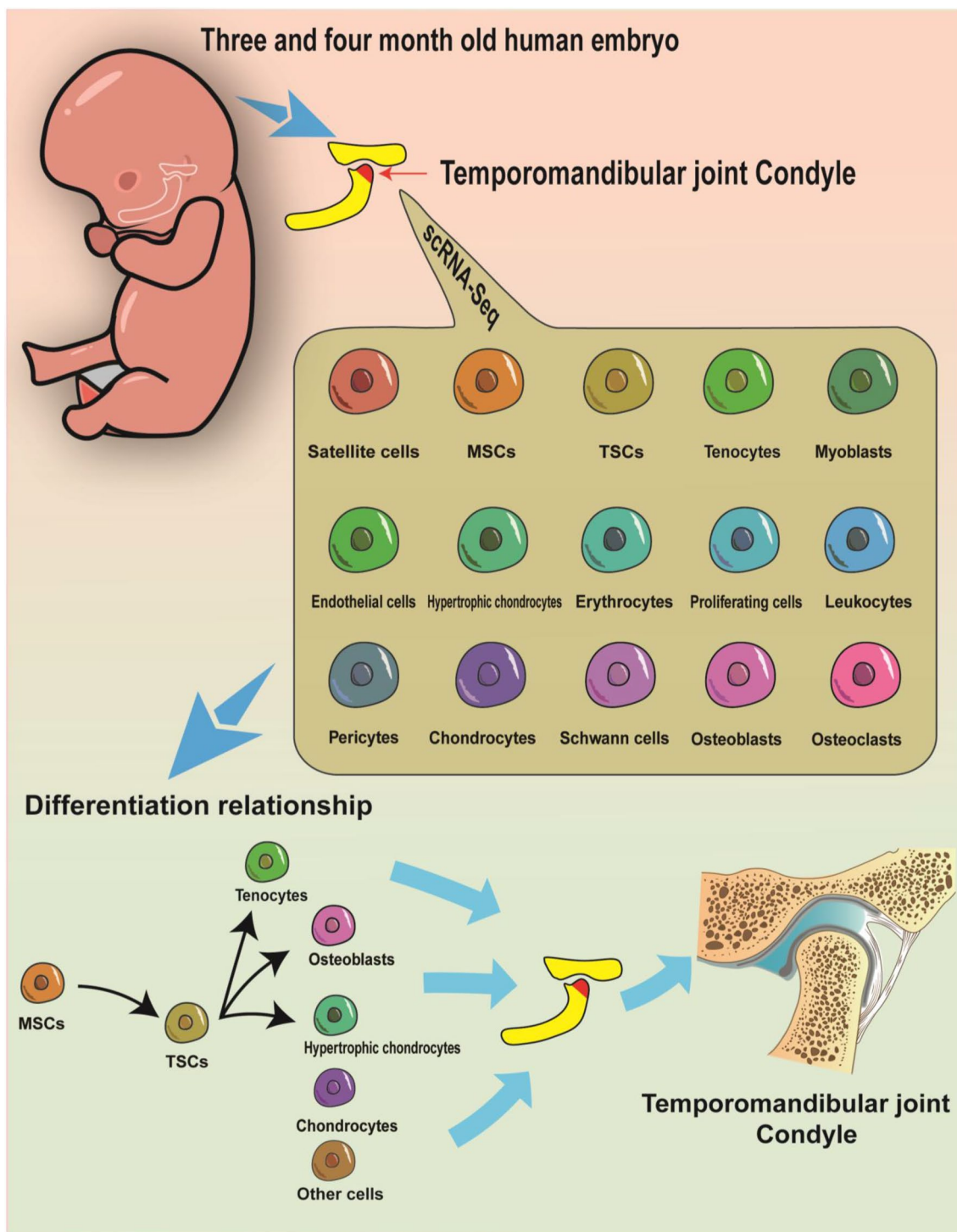


**Fig. 6** Overview of the cell types and differentiation relationship among human embryonic TMJC cells

Cell clusters were separated using “FindNeighbors” in 50 dimensions and “FindClusters” at a resolution of 0.25. Subcluster analyses of TSCs was set up using a resolution of 0.1. The clusters were visualized using the Uniform

Manifold Approximation and Projection (UMAP) algorithm. For the analysis of differentially expressed genes (DEGs), Seurat’s “FindMarkers” was used. Genes that were more than 25% expressed in their clusters and had

a mean log (Fold Change) greater than 0.25 were defined as DEGs.

#### Cell type annotation and gene enrichment analyses

Cell types were annotated based on the expression of marker genes known from published literature. Subsequently, gene enrichment was performed using clusterProfiler v3.6.1 (<https://bioconductor.org/packages/3.11/bioc/html/clusterProfiler.html>) [76]. Biological process (BP) with  $p_{adj}$  value  $< 0.05$  were defined as significantly enriched. GO classification was screened from the org.Hs.eg.db database (<https://bioconductor.org/packages/3.11/data/annotation/html/org.Hs.eg.db.html>).

#### Trajectory analysis and RNA velocity

The pseudotime trajectories of TMJC cell clusters were analyzed by Monocle 3 (<https://cole-trapnellab.github.io/monocle3>). Highly variable genes were selected from each cluster. Trajectories were visualized using the UMAP method. Finally, cells were sorted according to developmental and differentiation relationships. For RNA velocity analyses, the BAM file containing each cluster was first processed into a loom file. Subsequently, the loom files were processed as input into spliced and unspliced matrices. Finally, the results were visualized using the UMAP method.

#### Analysis of cell–cell communication

Cell–cell communication networks for ligand–receptor interaction were analyzed using CellChat (<http://www.cellchat.org/>; last accessed on May 10, 2021) [77]. A total of 32,491 ligand–receptor pairs were screened from the “CellChatDB.human” database. Using the “computeCommunProb” and “aggregateNet” in CellChat, the number of ligand–receptor interactions and the strength of interactions in the TMJC cell population were calculated. The “computeCommunProbPathway” function was used to determine the major signaling pathways. The outgoing communication patterns of secretory cells and the incoming communication patterns of target cells were analyzed using “identifyCommunicationPatterns” function.

#### Transcription factors analysis

Transcription factors were analyzed using a python version of Single-Cell Regulatory Network Inference and Clustering (pySCENIC) [78]. Cell-type-specific regulons were screened using the regulon specificity score (RSS) proposed in a previous study [79]. Regulon module analyses were performed using the Connection Specificity

Index (CSI) parameter which has been reported in previous studies [80]. Regulatory networks associated with MSCs and TSCs were analyzed using Cytoscape [81].

#### Immunofluorescent staining

The procedure for immunofluorescence was based on a previous studies [74]. Briefly, human embryonic TMJC was fixed in 4% paraformaldehyde for 24 h at 4 °C. The samples were demineralized at 4 °C gently shaking for 2 weeks in 4% EDTA in PBS. A 4- $\mu$ m-thick tissue section was cut from TMJC tissue. Antigen retrieval was performed using 10 mM sodium citrate buffer (pH 6.0). Sections were then blocked with 5% donkey serum containing 0.1% Triton X-100 in 2% BSA. Diluted primary antibodies were added to the sections and stored overnight at 4 °C. Sections were further incubated in the dark with the secondary antibody for 1 h at room temperature. Cell nuclei were stained with DAPI for 5 min. The images were captured with Leica SP8 laser scanning confocal microscopy (Leica TCSSP8, Leica).

The primary antibodies including Calpain 6 (10,120-1-AP, Proteintech), FGF2 (13,254-1-AP, Proteintech), SCIN (11,579-1-AP, Proteintech), CCR2 (16,153-1-AP, Proteintech), CYTL1 (15,856-1-AP, Proteintech), Calpain 6 (MA5-24,733, Invitrogen), PTN (27,117-1-AP, Proteintech), PTN (H00005764-M01, Novus Biologicals), THBS1 (PA5-102,583, Invitrogen), THBS1 (18,304-1-AP, Proteintech), were used in this study. The second antibodies including Alexa Fluor™ 488 (A-21206, Invitrogen) and Alexa Fluor™ 568 (A10037, Invitrogen) were used in this study.

#### Supplementary Information

The online version contains supplementary material available at <https://doi.org/10.1186/s13578-023-01069-5>.

**Additional file 1: Fig. S1.** Quality control of scRNA-seq and GO enrichment analysis. **a** The separation of TMJC. **b** The analysis of the number of genes, counts and percentage of mitochondria. **c** The statistics of cells in each cluster from 3 and 4-month-old human embryonic TMJC. **d** The marker genes for the annotation which were from pieces of literature. **e** The top five DEGs of each cluster in human embryonic TMJC. **f** GO analysis of each cluster in human embryonic TMJC. **g** The marker genes were used for the annotation of TSCs.

**Additional file 2: Fig. S2.** The immunofluorescent staining in 3 and 4-month-old human embryonic TMJC. **a** The expression of COL10A1, MMP13 and RUNX2 in each cluster of human embryonic TMJC. **b** The expression of FGF2 and SCIN in each cluster of human embryonic TMJC. **c** Immunofluorescence staining of FGF2 and SCIN in 3 and 4-month-old human embryonic TMJC, Scale bar = 1 mm and 50  $\mu$ m.

**Additional file 3: Fig. S3.** The differentiation relationship among human embryonic TMJC cells. **a** The differentiation relationship among 15 TMJC cell clusters based on Monocle3 analysis. **b** The RNA velocity analysis of 15 TMJC cell clusters. **c** The pseudotime analysis among MSCs, TSCs, tenocytes, hypertrophic chondrocytes and osteoblasts of the 3 and 4-month-old human embryonic TMJC. **d** The RNA velocity analysis among MSCs, TSCs, tenocytes, hypertrophic chondrocytes and osteoblasts of the 3 and 4-month-old human embryonic TMJC.

**Additional file 4: Fig. S4.** Cell Chat analysis of human embryonic TMJC cell clusters. **a** The interaction strength analysis of ligand-receptor pairs in 15 cell clusters. **b** FGF signaling pathway networks among 15 cell clusters. **c** The expression analysis of FGFR1 among 15 cell clusters. **d** FGF7-FGFR1 signaling pathway networks among 15 cell clusters. **e** The analysis of outgoing signaling patterns and incoming signaling patterns among 15 cell clusters.

**Additional file 5.**

**Additional file 6.**

### Acknowledgements

We thank all members of the laboratory for their experimental assistance and constructive discussions.

### Author contributions

Conceived and designed the experiments: XMF, JWS, DL and GFZ; Performed the experiments: QQZ, MYT, JPH, LL, RRJ, X.D.F and LW; Analyzed the data: CFW, HMX, JQZ, YJG, YQG; Wrote the paper: QQZ, MYT, and CNW.

### Funding

This work was supported by funds from the Nantong Science and Technology Project (MS12020030 to X.M.F), Shanghai Wu Mengchao Medical Science Foundation (HXKT20200019 to X.M.F), Jiangsu Yancheng Timstar Medical Technology Co. Natural Science Foundation (JC2021081 to J.W.S) partially supported by grants, Funing Mette Dental Material Factory (ZZXM-20201009 to X.M.F, ZZXM-20201008 to C.F.W), National Natural Science Foundation of China (2018YFA0801004 and 81870359 to D. L), Jiangsu Provincial Natural Science Foundation (BK20180048 and BRA2019278 to D.L), National Natural Science Foundation of China (82001606 to C.N.W), National Natural Science Foundation of China (82071838 to Z.F.G).

### Availability of data and materials

The raw data for this study are deposited in the Genome Sequence Archive [82] at the National Genomics Data Center for Biological Information/ National Genomics Data Center [83], Institute of Genomic Research, Chinese Academy of Sciences, Beijing, China (GSA-Human: HRA002545). The cell-gene matrix has been uploaded to "FigShare [<https://doi.org/10.6084/m9.figshare.20407371>], <https://doi.org/10.6084/m9.figshare.20407383>]. All other relevant data supporting the key findings of this study are available within the article and its Supplementary Information file, or from the corresponding author upon reasonable request.

### Code availability

All code associated with this manuscript have been uploaded to "GitHub [[https://github.com/qianqi234/human\\_embryonic\\_TMJ](https://github.com/qianqi234/human_embryonic_TMJ)]".

### Declarations

#### Ethics approval and consent to participate

This work was reviewed and approved by the Institutional Review Boards of Affiliated Hospital of Nantong University (2020-K013). Parents of study participants have signed an informed consent form.

#### Consent for publication

All authors agree to the submitted manuscript.

#### Competing interests

The authors declare no conflict of interest with this study.

#### Author details

<sup>1</sup>Department of Stomatology, Affiliated Hospital of Nantong University, Medical School of Nantong University, Nantong 226001, China. <sup>2</sup>Research Center of Clinical Medicine, Affiliated Hospital of Nantong University, Medical School of Nantong University, Nantong 226001, China. <sup>3</sup>Institute of Reproductive Medicine, Medical School of Nantong University, Nantong 226001, China. <sup>4</sup>School of Life Science, Nantong Laboratory of Development and Diseases Second Affiliated Hospital Key Laboratory of Neuroregeneration of Jiangsu

and Ministry of Education, Co-Innovation Center of Neuroregeneration, Nantong University, Nantong 226019, China.

Received: 11 January 2023 Accepted: 13 June 2023

Published online: 19 July 2023

### References

- Gauer RL, Semidey MJ. Diagnosis and treatment of temporomandibular disorders. *Am Fam Physician*. 2015;91(6):378–86.
- Stocum DL, Roberts WE. Part I: development and physiology of the temporomandibular joint. *Curr Osteoporos Rep*. 2018;16(4):360–8.
- Zarb GA, Carlsson GE. Temporomandibular disorders: osteoarthritis. *J Orofac Pain*. 1999;13(4):295–306.
- Bender ME, Lipin RB, Goudy SL. Development of the Pediatric Temporomandibular Joint. *Oral Maxillofac Surg Clin North Am*. 2018;30(1):1–9.
- Merida-Velasco JR, Rodriguez-Vazquez JF, Merida-Velasco JA, Sanchez-Montesinos I, Espin-Ferra J, Jimenez-Collado J. Development of the human temporomandibular joint. *Anat Rec*. 1999;255(1):20–33.
- Sunkara V, Heinz GA, Heinrich FF, Durek P, Mobasher A, Mashreghi MF, Lang A. Combining segmental bulk- and single-cell RNA-sequencing to define the chondrocyte gene expression signature in the murine knee joint. *Osteoarthr Cartil*. 2021;29(6):905–14.
- Wang X, Ning Y, Zhang P, Poulet B, Huang R, Gong Y, Hu M, Li C, Zhou R, Lammi MJ, et al. Comparison of the major cell populations among osteoarthritis, Kashin-Beck disease and healthy chondrocytes by single-cell RNA-seq analysis. *Cell Death Dis*. 2021;12(6):551.
- Mizoguchi F, Slowikowski K, Wei K, Marshall JL, Rao DA, Chang SK, Nguyen HN, Noss EH, Turner JD, Earp BE, et al. Functionally distinct disease-associated fibroblast subsets in rheumatoid arthritis. *Nat Commun*. 2018;9(1):789.
- Tang W, Li ZW, Miao GQ, Li ZP, Gui T, Wu CJ, Li ZY, Yang J, Zhao XD, Liu N, et al. Single-cell RNA sequencing reveals transcriptional changes in the cartilage of subchondral insufficiency fracture of the knee. *J Inflamm Res*. 2022;15:6105–12.
- Sebastian A, McCool JL, Hum NR, Muruges DK, Wilson SP, Christiansen BA, Loots GG. Single-cell RNA-Seq reveals transcriptomic heterogeneity and post-traumatic osteoarthritis-associated early molecular changes in mouse articular chondrocytes. *Cells*. 2021;10(6):1462.
- Karsenty G, Kronenberg HM, Settembre C. Genetic control of bone formation. *Annu Rev Cell Dev Biol*. 2009;25:629–48.
- Akiyama H, Kim JE, Nakashima K, Balmes G, Iwai N, Deng JM, Zhang Z, Martin JF, Behringer RR, Nakamura T, et al. Osteo-chondroprogenitor cells are derived from Sox9 expressing precursors. *Proc Natl Acad Sci U S A*. 2005;102(41):14665–70.
- Akiyama H, Chaboissier MC, Martin JF, Schedl A, de Crombrughe B. The transcription factor Sox9 has essential roles in successive steps of the chondrocyte differentiation pathway and is required for expression of Sox5 and Sox6. *Genes Dev*. 2002;16(21):2813–28.
- Hirata M, Kugimiya F, Fukai A, Saito T, Yano F, Ikeda T, Mabuchi A, Sapkota BR, Akune T, Nishida N, et al. C/EBPbeta and RUNX2 cooperate to degrade cartilage with MMP-13 as the target and HIF-2alpha as the inducer in chondrocytes. *Hum Mol Genet*. 2012;21(5):1111–23.
- Nakashima K, Zhou X, Kunkel G, Zhang Z, Deng JM, Behringer RR, de Crombrughe B. The novel zinc finger-containing transcription factor osterix is required for osteoblast differentiation and bone formation. *Cell*. 2002;108(1):17–29.
- Lum L, Beachy PA. The Hedgehog response network: sensors, switches, and routers. *Science*. 2004;304(5678):1755–9.
- Becher C, Szwart T, Ronstedt P, Ostermeier S, Skwara A, Fuchs-Winkelmann S, Tibesku CO. Decrease in the expression of the type 1 PTHrP receptor (PTH1R) on chondrocytes in animals with osteoarthritis. *J Orthop Surg Res*. 2010;5:28.
- Jin L, Gao F, Zhang L, Wang C, Hu L, Fan Z, Xia D. Pleiotropin enhances the osteo/dentinogenic differentiation potential of dental pulp stem cells. *Connect Tissue Res*. 2021;62(5):495–507.
- Zhu L, Liu Y, Wang A, Zhu Z, Li Y, Zhu C, Che Z, Liu T, Liu H, Huang L. Application of BMP in bone tissue engineering. *Front Bioeng Biotechnol*. 2022;10:810880.

20. Komori T. Regulation of proliferation, differentiation and functions of osteoblasts by Runx2. *Int J Mol Sci.* 2019;20(7):1694.
21. Liu C, Weng Y, Yuan T, Zhang H, Bai H, Li B, Yang D, Zhang R, He F, Yan S, et al. CXCL12/CXCR4 signal axis plays an important role in mediating bone morphogenetic protein 9-induced osteogenic differentiation of mesenchymal stem cells. *Int J Med Sci.* 2013;10(9):1181–92.
22. Suh J, Kim NK, Lee SH, Eom JH, Lee Y, Park JC, Woo KM, Baek JH, Kim JE, Ryou HM, et al. GDF11 promotes osteogenesis as opposed to MSTN, and follistatin, a MSTN/GDF11 inhibitor, increases muscle mass but weakens bone. *Proc Natl Acad Sci U S A.* 2020;117(9):4910–20.
23. Darvin P, Joung YH, Yang YM. JAK2-STAT5B pathway and osteoblast differentiation. *JAKSTAT.* 2013;2(4):e24931.
24. Kaneyama K, Segami N, Hatta T. Congenital deformities and developmental abnormalities of the mandibular condyle in the temporomandibular joint. *Congenit Anom.* 2008;48(3):118–25.
25. Cil AS, Bozkurt M, Bozkurt DK. Intrauterine temporomandibular joint dislocation: prenatal sonographic evaluation. *Clin Med Res.* 2014;12(1–2):58–60.
26. Dibbets JM, Carlson DS. Implications of temporomandibular disorders for facial growth and orthodontic treatment. *Semin Orthod.* 1995;1(4):258–72.
27. Ji Q, Zheng Y, Zhang G, Hu Y, Fan X, Hou Y, Wen L, Li L, Xu Y, Wang Y, et al. Single-cell RNA-seq analysis reveals the progression of human osteoarthritis. *Ann Rheum Dis.* 2019;78(1):100–10.
28. Kuo D, Ding J, Cohn IS, Zhang F, Wei K, Rao DA, Rozo C, Sokhi UK, Shanaj S, Oliver DJ, et al. HBEGF(+) macrophages in rheumatoid arthritis induce fibroblast invasiveness. *Sci Transl Med.* 2019;11:eaa8587.
29. Zhang F, Wei K, Slowikowski K, Fonseka CY, Rao DA, Kelly S, Goodman SM, Tabechian D, Hughes LB, Salomon-Escoto K, et al. Defining inflammatory cell states in rheumatoid arthritis joint synovial tissues by integrating single-cell transcriptomics and mass cytometry. *Nat Immunol.* 2019;20(7):928–42.
30. Stephenson W, Donlin LT, Butler A, Rozo C, Bracken B, Rashidfarrokhi A, Goodman SM, Ivashkiv LB, Bykerk VP, Orange DE, et al. Single-cell RNA-seq of rheumatoid arthritis synovial tissue using low-cost microfluidic instrumentation. *Nat Commun.* 2018;9(1):791.
31. Symons RA, Colella F, Collins FL, Rafipay AJ, Kania K, McClure JJ, White N, Cunningham I, Ashraf S, Hay E, et al. Targeting the IL-6-Yap-Snail signalling axis in synovial fibroblasts ameliorates inflammatory arthritis. *Ann Rheum Dis.* 2022;81(2):214–24.
32. Collins FL, Roelofs AJ, Symons RA, Kania K, Campbell E, Collie-Duguid ESR, Riemen AHK, Clark SM, De Bari C. Taxonomy of fibroblasts and progenitors in the synovial joint at single-cell resolution. *Ann Rheum Dis.* 2023;82(3):428–37.
33. Fang W, Sun Z, Chen X, Han B, Vangsness CT Jr. Synovial fluid mesenchymal stem cells for knee arthritis and cartilage defects: a review of the literature. *J Knee Surg.* 2021;34(13):1476–85.
34. Mackie EJ, Ahmed YA, Tatarczuch L, Chen KS, Mirams M. Endochondral ossification: how cartilage is converted into bone in the developing skeleton. *Int J Biochem Cell Biol.* 2008;40(1):46–62.
35. Qin X, Jiang Q, Nagano K, Moriishi T, Miyazaki T, Komori H, Ito K, Mark KV, Sakane C, Kaneko H, et al. Runx2 is essential for the transdifferentiation of chondrocytes into osteoblasts. *PLoS Genet.* 2020;16(11):e1009169.
36. Dalle Carbonare L, Bertacco J, Minoia A, Cominacini M, Bhandary L, Elia R, Gambaro G, Mottes M, Valenti MT. Modulation of miR-204 expression during chondrogenesis. *Int J Mol Sci.* 2022;23(4):2130.
37. Arai Y, Choi B, Kim BJ, Park S, Park H, Moon JJ, Lee SH. Cryptic ligand on collagen matrix unveiled by MMP13 accelerates bone tissue regeneration via MMP13/Integrin alpha3/RUNX2 feedback loop. *Acta Biomater.* 2021;125:219–30.
38. Delgado-Calle J, Sato AY, Bellido T. Role and mechanism of action of sclerostin in bone. *Bone.* 2017;96:29–37.
39. Wang X, Geng B, Wang H, Wang S, Zhao D, He J, Lu F, An J, Wang C, Xia Y. Fluid shear stress-induced down-regulation of microRNA-140-5p promotes osteoblast proliferation by targeting VEGFA via the ERK5 pathway. *Connect Tissue Res.* 2022;63(2):156–68.
40. Bian H, Zhu T, Liang Y, Hei R, Zhang X, Li X, Chen J, Lu Y, Gu J, Qiao L, et al. Expression profiling and functional analysis of candidate Col10a1 regulators identified by the TRAP program. *Front Genet.* 2021;12:683939.
41. Nishikawa K, Nakashima T, Takeda S, Isogai M, Hamada M, Kimura A, Kodama T, Yamaguchi A, Owen MJ, Takahashi S, et al. Maf promotes osteoblast differentiation in mice by mediating the age-related switch in mesenchymal cell differentiation. *J Clin Invest.* 2010;120(10):3455–65.
42. Liu Y, Monticone M, Tonachini L, Mastrogiacomo M, Marigo V, Cancedda R, Castagnola P. URB expression in human bone marrow stromal cells and during mouse development. *Biochem Biophys Res Commun.* 2004;322(2):497–507.
43. Mross C, Marko M, Munck M, Glockner G, Motameny S, Altmuller J, Noegel AA, Eichinger L, Peche VS, Neumann S. Depletion of nesprin-2 is associated with an embryonic lethal phenotype in mice. *Nucleus.* 2018;9(1):503–15.
44. Poudel SB, Bhattarai G, Kim JH, Kook SH, Seo YK, Jeon YM, Lee JC. Local delivery of recombinant human FGF7 enhances bone formation in rat mandible defects. *J Bone Miner Metab.* 2017;35(5):485–96.
45. Jeon YM, Kook SH, Rho SJ, Lim SS, Choi KC, Kim HS, Kim JG, Lee JC. Fibroblast growth factor-7 facilitates osteogenic differentiation of embryonic stem cells through the activation of ERK/Runx2 signaling. *Mol Cell Biochem.* 2013;382(1–2):37–45.
46. Tucker RP, Degen M. The expression and possible functions of tenascin-w during development and disease. *Front Cell Dev Biol.* 2019;7:53.
47. Omi M, Kaartinen V, Mishina Y. Activin A receptor type 1-mediated BMP signaling regulates RANKL-induced osteoclastogenesis via canonical SMAD-signaling pathway. *J Biol Chem.* 2019;294(47):17818–36.
48. Yan X, Fan DY, Pi YL, Zhang YN, Fu PJ, Zhang HF. ERalpha/beta/DMP1 axis promotes trans-differentiation of chondrocytes to bone cells through GSK-3beta/beta-catenin pathway. *J Anat.* 2022;240(6):1152–1161.
49. Xu C, Zhu S, Wu M, Han W, Yu Y. Functional receptors and intracellular signal pathways of midkine (MK) and pleiotrophin (PTN). *Biol Pharm Bull.* 2014;37(4):511–20.
50. Noguchi T, Ebina K, Hirao M, Kawase R, Ohama T, Yamashita S, Morimoto T, Koizumi K, Kitaguchi K, Matsuoka H, et al. Progranulin plays crucial roles in preserving bone mass by inhibiting TNF-alpha-induced osteoclastogenesis and promoting osteoblastic differentiation in mice. *Biochem Biophys Res Commun.* 2015;465(3):638–43.
51. Gross S, Krause Y, Wuelling M, Vortkamp A. Hoxa11 and Hoxd11 regulate chondrocyte differentiation upstream of Runx2 and Shox2 in mice. *PLoS ONE.* 2012;7(8):e43553.
52. Haraguchi R, Kitazawa R, Kitazawa S. Epigenetic regulation of Tbx18 gene expression during endochondral bone formation. *Cell Tissue Res.* 2015;359(2):503–12.
53. Rodrigo I, Hill RE, Balling R, Munsterberg A, Imai K. Pax1 and Pax9 activate Bapx1 to induce chondrogenic differentiation in the sclerotome. *Development.* 2003;130(3):473–82.
54. Komori T. Regulation of osteoblast differentiation by transcription factors. *J Cell Biochem.* 2006;99(5):1233–9.
55. Zhou S, Dai Q, Huang X, Jin A, Yang Y, Gong X, Xu H, Gao X, Jiang L. STAT3 is critical for skeletal development and bone homeostasis by regulating osteogenesis. *Nat Commun.* 2021;12(1):6891.
56. Chen G, Fan D, Zhang W, Wang S, Gu J, Gao Y, He L, Li W, Zhang C, Li M, et al. Mxk mediates tenogenic differentiation but incompletely inhibits the proliferation of hypoxic MSCs. *Stem Cell Res Ther.* 2021;12(1):426.
57. Bell N, Bhagat S, Muruganandan S, Kim R, Ho K, Pierce R, Kozhemyakina E, Lassar AB, Gamer L, Rosen V, et al. Overexpression of transcription factor FoxA2 in the developing skeleton causes an enlargement of the cartilage hypertrophic zone, but it does not trigger ectopic differentiation in immature chondrocytes. *Bone.* 2022;160:116418.
58. Michikami I, Fukushi T, Honma S, Yoshioka S, Itoh S, Muragaki Y, Kurisu K, Ooshima T, Wakisaka S, Abe M. Trps1 is necessary for normal temporomandibular joint development. *Cell Tissue Res.* 2012;348(1):131–40.
59. Yang Z, Ren Z, She R, Ao J, Wa Q, Sun Z, Li B, Tian X. miR-23a-3p regulated by LncRNA SNHG5 suppresses the chondrogenic differentiation of human adipose-derived stem cells via targeting SOX6/SOX5. *Cell Tissue Res.* 2021;383(2):723–33.
60. Amano K, Densmore M, Nishimura R, Lanske B. Indian hedgehog signaling regulates transcription and expression of collagen type X via Runx2/Smads interactions. *J Biol Chem.* 2014;289(36):24898–910.
61. Lee SH, Oh KN, Han Y, Choi YH, Lee KY. Estrogen receptor alpha regulates Dlx3-mediated osteoblast differentiation. *Mol Cells.* 2016;39(2):156–62.
62. Tan Z, Kong M, Wen S, Tsang KY, Niu B, Hartmann C, Chan D, Hui CC, Cheah KSE. IRX3 and IRX5 Inhibit adipogenic differentiation of hypertrophic chondrocytes and promote osteogenesis. *J Bone Miner Res.* 2020;35(12):2444–57.

63. Vogiatzi A, Baltsavia I, Dialyans E, Theodorou V, Zhou Y, Deligianni E, Iliopoulos I, Wilkie AOM, Twigg SRF, Mavrothalassitis G. Erf affects commitment and differentiation of osteoprogenitor cells in cranial sutures via the retinoic acid pathway. *Mol Cell Biol*. 2021;41(8):e0014921.
64. Zhang L, Liu Y, Feng B, Liu LG, Zhou YC, Tang H. MiR-138-5p knock-down promotes osteogenic differentiation through FOXC1 up-regulation in human bone mesenchymal stem cells. *Biochem Cell Biol*. 2021;99(3):296–303.
65. Zhang H, Xu R, Li B, Xin Z, Ling Z, Zhu W, Li X, Zhang P, Fu Y, Chen J, et al. LncRNA NEAT1 controls the lineage fates of BMSCs during skeletal aging by impairing mitochondrial function and pluripotency maintenance. *Cell Death Differ*. 2022;29(2):351–65.
66. Herlofsen SR, Hoiby T, Cacchiarelli D, Zhang X, Mikkelsen TS, Brinchmann JE. Brief report: importance of SOX8 for in vitro chondrogenic differentiation of human mesenchymal stromal cells. *Stem Cells*. 2014;32(6):1629–35.
67. Auld KL, Berasi SP, Liu Y, Cain M, Zhang Y, Huard C, Fukayama S, Zhang J, Choe S, Zhong W, et al. Estrogen-related receptor alpha regulates osteoblast differentiation via Wnt/beta-catenin signaling. *J Mol Endocrinol*. 2012;48(2):177–91.
68. Mikasa M, Rokutanda S, Komori H, Ito K, Tsang YS, Date Y, Yoshida CA, Komori T. Regulation of Tcf7 by Runx2 in chondrocyte maturation and proliferation. *J Bone Miner Metab*. 2011;29(3):291–9.
69. Sivakamasundari V, Kraus P, Sun W, Hu X, Lim SL, Prabhakar S, Lufkin T. A developmental transcriptomic analysis of Pax1 and Pax9 in embryonic intervertebral disc development. *Biol Open*. 2017;6(2):187–99.
70. Liu Z, Wang H, Hou Y, Yang Y, Jia J, Wu J, Zuo Z, Gao T, Ren S, Bian Y, et al. CNC-bZIP protein NFE2L1 regulates osteoclast differentiation in antioxidant-dependent and independent manners. *Redox Biol*. 2021;48:102180.
71. Pastore N, Huynh T, Herz NJ, Calcagni A, Klisch TJ, Brunetti L, Kim KH, De Giorgi M, Hurley A, Carissimo A, et al. TFEB regulates murine liver cell fate during development and regeneration. *Nat Commun*. 2020;11(1):2461.
72. Antonopoulou I, Mavrogiannis LA, Wilkie AO, Morriss-Kay GM. Alx4 and Msx2 play phenotypically similar and additive roles in skull vault differentiation. *J Anat*. 2004;204(6):487–99.
73. Zeng X, Wang Y, Dong Q, Ma MX, Liu XD. DLX2 activates Wnt1 transcription and mediates Wnt/beta-catenin signal to promote osteogenic differentiation of hBMSCs. *Gene*. 2020;744: 144564.
74. Shi J, Fok KL, Dai P, Qiao F, Zhang M, Liu H, Sang M, Ye M, Liu Y, Zhou Y, et al. Spatio-temporal landscape of mouse epididymal cells and specific mitochondria-rich segments defined by large-scale single-cell RNA-seq. *Cell Discov*. 2021;7(1):34.
75. Stuart T, Butler A, Hoffman P, Hafemeister C, Papalexi E, Mauck WM 3rd, Hao Y, Stoeckius M, Smibert P, Satija R. Comprehensive integration of single-cell data. *Cell*. 2019;177(7):1888–1902 e1821.
76. Yu G, Wang LG, Han Y, He QY. clusterProfiler: an R package for comparing biological themes among gene clusters. *OMICS*. 2012;16(5):284–7.
77. Jin S, Guerrero-Juarez CF, Zhang L, Chang I, Ramos R, Kuan CH, Myung P, Plikus MV, Nie Q. Inference and analysis of cell-cell communication using cell chat. *Nat Commun*. 2021;12(1):1088.
78. Aibar S, Gonzalez-Blas CB, Moerman T, Huynh-Thu VA, Imrichova H, Hulselmans G, Rambow F, Marine JC, Geurts P, Aerts J, et al. SCENIC: single-cell regulatory network inference and clustering. *Nat Methods*. 2017;14(11):1083–6.
79. Suo S, Zhu Q, Saadatpour A, Fei L, Guo G, Yuan GC. Revealing the critical regulators of cell identity in the mouse cell atlas. *Cell Rep*. 2018;25(6):1436–1445 e1433.
80. Fuxman Bass JI, Diallo A, Nelson J, Soto JM, Myers CL, Walhout AJ. Using networks to measure similarity between genes: association index selection. *Nat Methods*. 2013;10(12):1169–76.
81. Shannon P, Markiel A, Ozier O, Baliga NS, Wang JT, Ramage D, Amin N, Schwikowski B, Ideker T. Cytoscape: a software environment for integrated models of biomolecular interaction networks. *Genome Res*. 2003;13(11):2498–504.
82. Chen T, Chen X, Zhang S, Zhu J, Tang B, Wang A, Dong L, Zhang Z, Yu C, Sun Y, et al. The genome sequence archive family: toward explosive data growth and diverse data types. *Genom Proteom Bioinform*. 2021;19(4):578–83.
83. Members C-N, Partners. Database Resources of the National Genomics Data Center, China National Center for Bioinformatics in 2021. *Nucleic Acids Res*. 2021;49(D1):D18–28.

## Publisher's Note

Springer Nature remains neutral with regard to jurisdictional claims in published maps and institutional affiliations.

Ready to submit your research? Choose BMC and benefit from:

- fast, convenient online submission
- thorough peer review by experienced researchers in your field
- rapid publication on acceptance
- support for research data, including large and complex data types
- gold Open Access which fosters wider collaboration and increased citations
- maximum visibility for your research: over 100M website views per year

At BMC, research is always in progress.

Learn more [biomedcentral.com/submissions](https://biomedcentral.com/submissions)

